Macromolecules

ARTICLE

pubs.acs.org/Macromolecules

Side-Chain Architectures of 2,7-Carbazole and Quinoxaline-Based Polymers for Efficient Polymer Solar Cells

Ergang Wang,*,† Lintao Hou,‡ Zhongqiang Wang,‡ Zaifei Ma,‡ Stefan Hellström,† Wenliu Zhuang,† Fengling Zhang,‡ Olle Inganäs,‡ and Mats R. Andersson*,†

†Department of Chemical and Biological Engineering/Polymer Technology, Chalmers University of Technology, SE-412 96 Göteborg, Sweden

‡Biomolecular and Organic Electronics, IFM, Linköping University, SE-581 83 Linköping, Sweden

ABSTRACT: Three polymers bearing a common carbazole−thiophene−quinoxaline−thiophene backbone, but different side chains, were designed and synthesized in order to investigate the effect of side chains on their photovoltaic performance. Their photophysical, electrochemical, and photovoltaic properties were investigated and compared. The polymer **EWC3**, with the largest amount of side chains, showed the highest power conversion efficiency of 3.7% with an open-circuit voltage (V_{oc}) of 0.92 V. The atomic force microscopy images of the active layers of the devices showed that the morphology was highly influenced by the choice of the solvent and processing additive. It is worth noting that polymer solar cells (PSCs) fabricated from **EWC3**, with branched side chains on the carbazole units, gave a much higher V_{oc} than the devices made from **EWC1**, which bears the same electron-deficient segment as **EWC3** but straight side chains on carbazole units. This study offered a useful and important guideline for designing 2,7-carbazole-based polymers for high-performance PSCs.

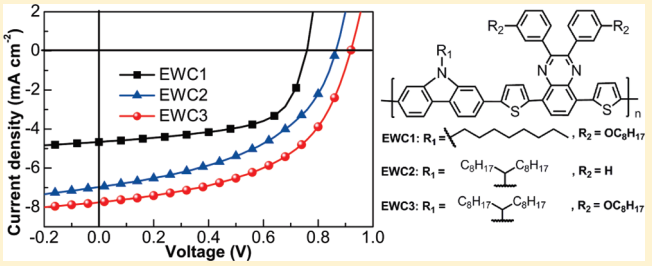

INTRODUCTION

Renewable energy sources are regarded as key technologies to solve the world energy crisis. Polymer solar cells (PSCs) are promising sustainable solar energy converters, which are attracting more and more attention because of their unique advantages of low cost, light weight, and potential use in flexible devices.[1−4] Based on the concept of bulk heterojunction (BHJ) structure,[5] PSCs made by blending poly(3-hexylthiophene) (P3HT) as donor and [6,6]-phenyl-C_{61}-butyric acid methyl ester ([60]PCBM) as acceptor were intensively investigated, leading to power conversion efficiencies (PCEs) up to 4−5%.[6,7] Yet, the PCEs of P3HT-based solar cells were mainly limited by their narrow absorption spectra ranging from 300 to 650 nm.[8,9] Therefore, a wide array of low-band-gap polymers were developed to serve as the active layers in PSCs aiming at matching their absorptions well with the solar radiation spectrum. Recently, great progress has been achieved in improving the performances of PSCs with efficiencies reaching over 7%.[10,11]

A facile method to achieve low-band-gap polymers by combining electron-rich (donor) and electron-deficient (acceptor) moieties in their repeating units, forming internal donor−acceptor (D−A) structures, was intensively investigated.[10−15] This strategy helped to develop the most efficient donor polymers for PSCs.[10,11] 2,7-Functionalized carbazole proved to be an excellent donor unit in a class of polymers with PCEs over 6%.[10,16] The appropriate choice of electron-deficient units as acceptors is of paramount importance to achieve low-band-gap polymers for highly efficient solar cells. Quinoxaline-containing segments were shown to be promising acceptors when combined with fluorene or thiophene (as donor) forming D−A polymers.[17−19] It is therefore worth studying the photovoltaic performances of D−A polymers with 2,7-carbazole as donor and quinoxaline segments as acceptor. In this article, we report the synthesis and characterization of a series of D−A copolymers based on 2,7-carbazole and quinoxaline segments. Very recently, a similar polymer was reported, which showed a PCE of 2.2% in PSCs.[20]

Alkyl or alkoxy side chains are commonly incorporated on the backbones of D−A polymers to ensure high solubility and to allow solution processing. It was found that the proper placement of alkyl or alkoxy groups is important, and this can have pronounced effect on the performance of the resulting PSCs.[21−28] To gain more insight into the influence of alkyl or alkoxy groups in the photophysical, electrochemical, and photovoltaic properties of 2,7-carbazole-based polymers, we designed and synthesized three polymers (**EWC1**, **EWC2**, and **EWC3**) with a common carbazole−thiophene−quinoxaline−thiophene backbone but with different side chains. The devices based on **EWC3** showed the best performance with a PCE of 3.7%.

RESULTS AND DISCUSSION

Material Synthesis. The chemical structures and synthetic routes toward the three polymers are outlined in Scheme 1. The

Received: December 7, 2010
Revised: February 7, 2011
Published: March 07, 2011

Scheme 1. Synthetic Routes of the Three Polymers

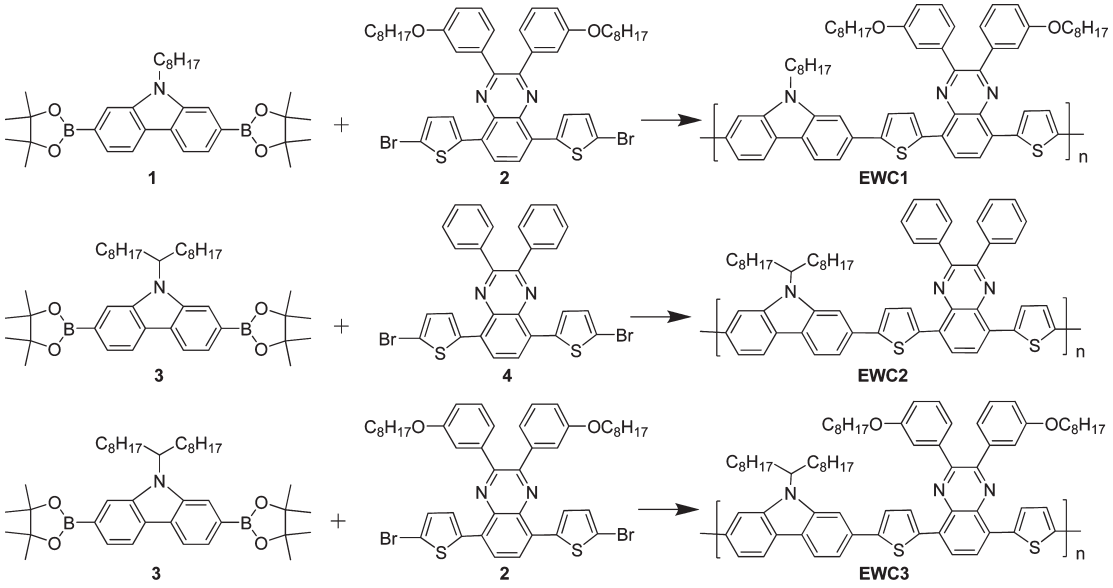

monomers 9-octyl-2,7-bis(4,4,5,5-tetramethyl-1,3,2-dioxaborolan-2-yl)-9*H*-carbazole (**1**), 5,8-bis(5-bromothiophen-2-yl)-2,3-bis(3-(octyloxy)phenyl)quinoxaline (**2**), 9-(heptadecan-9-yl)-2,7-bis(4,4,5,5-tetramethyl-1,3,2-dioxaborolan-2-yl)-9*H*-carbazole (**3**), and 5,8-bis(5-bromothiophen-2-yl)-2,3-diphenylquinoxaline (**4**) were synthesized according to modified literature procedures.[15,18,29] All three polymers were obtained by coupling the corresponding carbazole-based and quinoxaline-based monomers via a modified Suzuki reaction.[19,30] The polymerizations were carried out by applying almost the same conditions, but the reaction times for **EWC1** and **EWC2** were much shorter than for **EWC3** due to the lower number of side chains and limited solubility. Precipitation was observed after the reaction proceeded for 4 h for **EWC1** and 2 h for **EWC2**. To limit the molecular weights and gain in the amount of soluble polymers of **EWC1** and **EWC2**, end-capping was carried out as soon as precipitation occurred. Size exclusion chromatography (SEC) was employed to measure the molecular weights of the polymers using a polystyrene calibration. **EWC2**, with only two side chains in its repeating unit, showed the lowest number-averaged molecular weight (M_n) of 9000 with polydispersity index (PDI) of 1.7. **EWC3**, which possessed the most side chains on its backbone, exhibited much better solubility and higher molecular weight with M_n of 23 000 and PDI of 2.7. However, **EWC1**, containing three side chains in its repeating unit, exhibited the highest molecular weight with M_n of 34 000 and PDI of 2.9. The influence of the number of side chains on the solubilities and molecular weights of the resulting polymers is strong. To remove the catalyst residue and reduce their influence in the performance of the resulting solar cells, all three polymers were purified carefully by washing with sodium diethyldithiocarbamate trihydrate solution and then by Soxhlet extraction with diethyl ether and chloroform.[31,32] It was noted that the SEC spectrum of **EWC1** presents two peaks resulting in low M_n of 14 000 and large PDI of 7.3 if it was washed in the Soxhlet extractor using diethyl ether and then extracted with chloroform. With regard to this unusual PDI, we decided to wash it by using

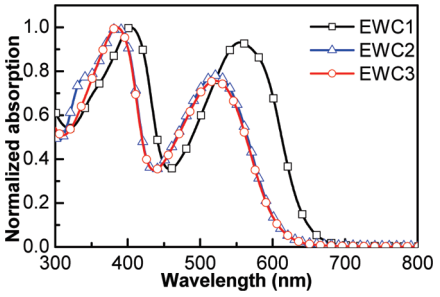

Figure 1. UV−vis absorption spectra of the polymers in chloroform solution.

dichloromethane as eluent after using diethyl ether. After that, the high-molecular-weight fraction in the thimble was Soxhlet-extracted by chloroform. In this case, the low molecular weight fraction of **EWC1** was remove by dichloromethane, leading to an improved of M_n of 34 000 and narrowed PDI of 2.9.

Thermogravimetric analysis (TGA) was used to investigate the thermal stabilities of the polymers. All three polymers exhibited excellent stability with degradation temperatures over 400 °C (5% weight loss). **EWC2** showed a glass transition temperature (T_g) of 114 °C measured by differential scanning calorimetry (DSC), which is much higher than that of **EWC3** (T_g = 68 °C). This difference can be attributed to the lower number of side chains in **EWC2**, which leads to tightly arranged polymer chains and limited movement of chain segments. No thermal transition could be detected for **EWC1** between 20 and 250 °C, which can be tentatively attributed to its compact configuration due to the straight side chains on carbazole units.

Optical and Electrochemical Properties. The UV−vis absorption spectra of the polymers in chloroform solution and in the solid state are shown in Figures 1 and 2, respectively. All three polymers present two absorption bands. The band at shorter wavelength originates from the carbazole segments, and the band at longer wavelength can be attributed to intramolecular charge

transfer (ICT). **EWC2** and **EWC3** showed a less pronounced ICT compared to their polyfluorene-based analogues APFO-18 and APFO-15.[18] The almost identical absorption spectra of **EWC2** and **EWC3**, both in solution and in the solid state, respectively, indicate that the octyloxy groups on the quinoxaline segments of **EWC3** have no influence in the absorption spectrum of the resulting polymers. In contrast, the side chains on the carbazole units have an obvious effect on the absorption spectra of the resulting polymers, which can be seen from the fact that **EWC1** with absorption onset of 680 nm and optical band gap (E_g^{op}) of 1.82 eV showed a visible red shift compared to **EWC3** with absorption onset of 644 nm and E_g^{op} of 1.92 eV. The absorption maxima and E_g^{op} of the polymers estimated from the absorption onset are summarized in Table 1. It was noted that there is only very limited red shift for the absorption spectra of all the synthesized polymers when going from the solution to the solid state, indicating that the polymers are amorphous, and there is no obvious aggregation or long-range orderly $\pi-\pi$ stacking formed in the solid state.

The positions of the highest occupied molecular orbital (HOMO) and lowest unoccupied molecular orbital (LUMO) of the polymers are key parameters for the performance of the resulting PSCs, which can affect the driving force for charge transfer and the V_{oc}.[33] The HOMO and LUMO positions can be estimated from the oxidation and reduction potentials obtained in electrochemical measurements. Square-wave voltammetry (SWV)[18,34] was used to determine the oxidation and reduction potentials of the polymers instead of the traditional cyclic voltammetry,[21,35] as SWV is more sensitive and more convenient to define the oxidation and reduction potentials based on the much clearer peaks in the voltammograms. As shown in Figure 3, the square-wave voltammograms of the three polymers present almost the same reduction potentials of ca. −1.8 V, but different oxidation potentials. The HOMO and LUMO levels were calculated according to the formula HOMO = $-(E^{ox} + 5.13)$ eV and LUMO = $-(E^{red} + 5.13)$ eV, by setting the oxidative peak potential of ferrocene/ferrocenium (Fc/Fc^+) vs the normal-hydrogen electrode (NHE) to 0.63 V[36] and the NHE energy level relative to vacuum to 4.5 eV.[37] The relative electrochemical parameters and estimated HOMO/LUMO levels of the polymers are listed in Table 1. For comparison, the reduction potential of [70]PCBM ([6,6]-phenyl-C_{71}-butyric acid methyl ester) was measured to be −1.00 V by SWV under the same conditions, and its LUMO level was calculated to be −4.13 eV. The high LUMO levels of the three polymers can ensure enough driving force for charge transfer in the resulting PSCs utilizing [70]PCBM as acceptor.[33] As the V_{oc} of the resulting PSCs is linearly correlated to the difference between the LUMO level of acceptors and HOMO level of donor polymers, the deeper HOMO level of **EWC3** indicates its higher V_{oc} in solar cells compared to the other two polymers.[33] The relatively higher HOMO level of **EWC1** was tentatively explained by its compact configuration due to the straight side chains on the carbazole segments, which is also indicated by its red-shifted absorption spectrum mentioned above (see Figure 2). On the basis of the above data, it was concluded that the side chains on both carbazole and quinoxaline segments have no influence on the LUMO levels of the polymers but a clear impact on their HOMO levels.

Photovoltaic Properties. To investigate the photovoltaic properties of the polymers, solar cells with a sandwich configuration of glass/ITO/PEDOT:PSS/active layer/LiF/Al were fabricated. The active layers of the solar cells were spin-coated from *o*-dichlorobenzene (ODCB) solutions of polymer:[70]PCBM. [70]PCBM was chosen as the electron acceptor instead of [60]PCBM because [70]PCBM has similar electronic properties to [60]PCBM but a considerably higher absorption coefficient in the visible region.[38] The ratio of polymer:[70]PCBM is an important parameter, which has a pronounced influence in the performance of the resulting PSCs.[14] Thus, solar cell devices were fabricated from each polymer with weight ratios of polymer:[70]PCBM varying from 1:1, 1:2, 1:3 to 1:4. The results of the photovoltaic performances of these devices and their corresponding active-layer thicknesses are listed in Table 2. All three polymers achieved their best performances with polymer:[70]PCBM ratio of 1:3. The corresponding current density−voltage ($J-V$) curves of the 1:3 devices, under illumi-

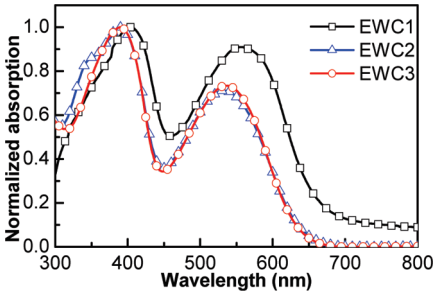

Figure 2. UV−vis absorption spectra of the polymers in the solid state.

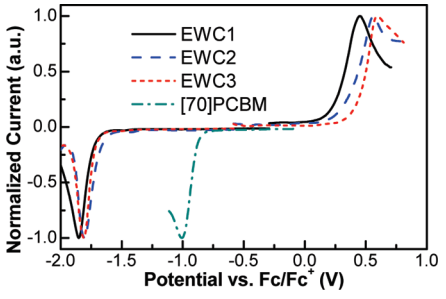

Figure 3. Square wave voltammograms of the polymers and [70]PCBM in film.

Table 1. Optical and Electrochemical Properties of the Polymers

	λ_{max} (nm)							
polymer	solution	film	λ_{onset} (nm) film	E_g^{op} (eV)	E^{ox} (V)	E^{red} (V)	HOMO (eV)	LUMO (eV)
EWC1	405, 554	404, 558	680	1.82	0.43	−1.84	−5.56	−3.29
EWC2	386, 521	390, 533	649	1.91	0.56	−1.80	−5.69	−3.33
EWC3	385, 521	390, 536	644	1.92	0.60	−1.81	−5.73	−3.32

dx.doi.org/10.1021/ma102783d |*Macromolecules* 2011, 44, 2067–2073

nation of AM 1.5G simulated solar light (100 mW cm^{-2}), are shown in Figure 4. To validate the measurements, the corresponding external quantum efficiencies (EQEs) were measured under illumination of monochromatic light. All current density (J_{sc}) values calculated from integration of the EQEs of the devices, with an AM 1.5G reference spectrum, agree well with the J_{sc} values obtained from the $J-V$ measurements. The EQE profiles from all three polymers present shallower valleys at 400−500 nm compared to the corresponding absorption spectra, indicating that both the absorptions of the polymers and [70]PCBM contribute to the photocurrents of the resulting devices. **EWC3** exhibited the highest PCE of 3.7% with V_{oc} of 0.92 V, J_{sc} of 7.7 mA cm^{-2}, and fill factor of 0.52. It was noted that

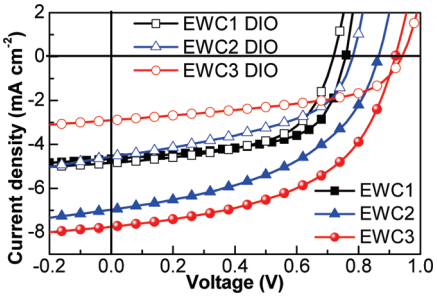

Figure 4. $J-V$ curves of the devices from the three polymers (polymer:[70]PCBM ratio of 1:3) processed with (open symbol) and without (solid symbol) DIO as processing additive.

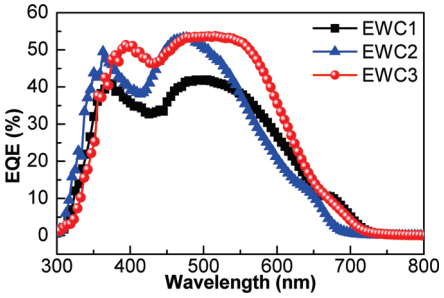

Figure 5. EQE of the devices from the three polymers (polymer:[70]-PCBM ratio of 1:3) processed without additive.

the V_{oc} of devices fabricated from the three polymers decrease by ca. 0.1 V with increasing amounts of [70]PCBM. The devices from **EWC3** exhibited higher V_{oc}, which is consistent with its deeper HOMO level.[33] With the polymer:[70]PCBM ratio of 1:3, devices from **EWC3**, with branched side chains on carbazole segments, exhibited 0.17 V higher V_{oc} values than devices made of **EWC1**, with straight side chains on carbazole segments. This kind of direct comparison between 2,7-carbazole-based polymers with branched and straight side chains on the carbazole moieties[15,39,40] bearing the same acceptor segments was rarely noted before. It is striking to find that branched side chains on the carbazole units are beneficial in achieving higher V_{oc} in the resulting devices. This result is consistent with the recent reports about the effect of side chains based on other polymer backbones, and it is believed that branched side chains can reduce intermolecular interaction and lead to higher V_{oc}.[26,27,41] This observation may be of importance in the designing of carbazole-based polymers for high-efficiency PSCs.

The nanostructure of the active layer can influence charge separation and transport and is very important for the performance of a PSC.[42] It was found that processing additives and mixing solvents have considerable influence on the morphology of the active layers and then the performances of the devices.[40,42−44] Here, we chose 1,8-diiodooctane (DIO) as additive to investigate its effect on the performance of the three polymers with different side chains. DIO (2.5 vol %) was added to the solution of polymer:[70]PCBM (1:3) in ODCB, and then the resulting solution was spin-coated onto PEDOT:PSS layer as active layer. However, all devices fabricated from the three polymers, processed with DIO as additive, exhibited lower performances. The $J-V$ curves of these devices are shown in Figure 4, and the relative photovoltaic parameters are summarized in Table 2. To look into the reason for the lower performance, the morphologies of the active layers processed with and without additive were investigated by atomic force microscopy (AFM). As shown in Figure 6, the AFM height images (scan area $2 \times 2\ \mu m^2$) of **EWC2**:[70]PCBM and **EWC3**:[70]PCBM, spin-coated from ODCB without additive, presented smooth films and small domain sizes with root-mean-square (rms) surface roughness of 0.4 and 1.9 nm, respectively (Figure 6c,e). In contrast, the images from the two blends processed with additive exhibited rough films and much larger domain sizes with rms

Table 2. Photovoltaic Parameters of the Solar Cells from the Three Polymers

polymer	additive	weight ratio polymer:[70]PCBM	thickness (nm)	V_{oc} (V)	J_{sc} (mA cm^{-2})	FF	PCE (%)
EWC1	none	1:1	60	0.74	3.8	0.58	1.7
		1:2	65	0.75	5.4	0.55	2.2
		1:3	65	0.75	4.7	0.60	2.2
		1:4	60	0.73	4.2	0.60	2.0
	DIO	1:3	65	0.72	4.7	0.55	1.9
EWC2	none	1:1	80	0.90	6.9	0.44	2.7
		1:2	65	0.85	6.9	0.53	3.1
		1:3	60	0.81	7.1	0.54	3.1
		1:4	95	0.80	7.1	0.51	2.9
	DIO	1:3	70	0.79	4.3	0.54	1.9
EWC3	none	1:1	85	0.96	5.7	0.37	2.1
		1:2	95	0.92	6.1	0.46	2.6
		1:3	70	0.92	7.7	0.52	3.7
		1:4	85	0.87	7.0	0.48	2.9
	DIO	1:3	70	0.94	2.7	0.57	1.4

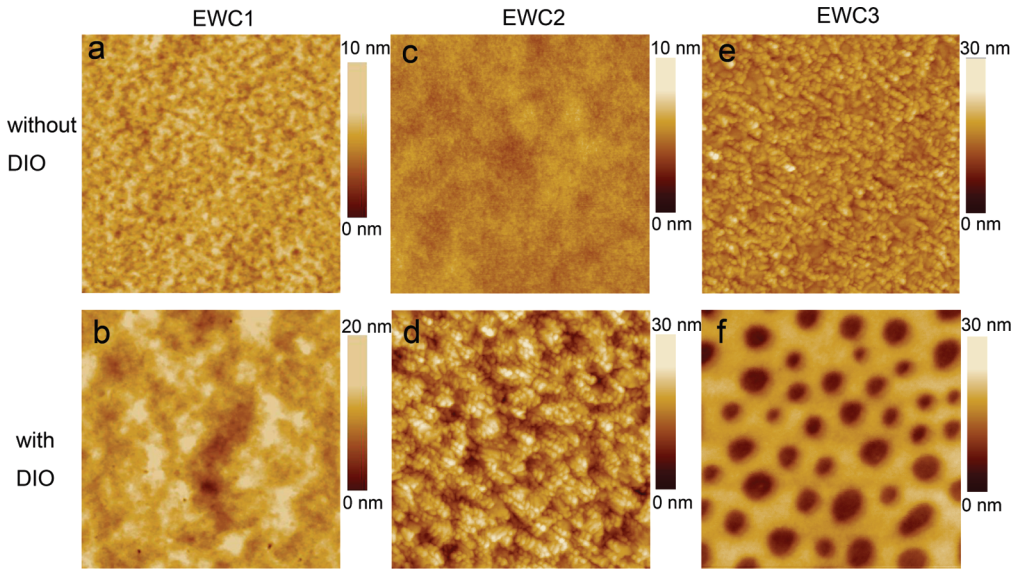

Figure 6. AFM images ($2 \times 2\ \mu m^2$) of the active layers from the three polymers (polymer:[70]PCBM ratio of 1:3) processed with (bottom) and without (up) additive.

surface roughness of 3.4 and 3.9 nm (Figure 6d,f), respectively, indicating large phase separation took place. Large phase separation reduces the area for charge separation and increases the exciton diffusion length and the recombination of charges, leading to low photocurrent.[42,45] On the contrary, the devices fabricated from **EWC1** by processing with and without additive showed almost the same performances, which can be explained by their similar morphologies of the active layers with rms roughness of 1.9 nm (with additive, Figure 6b) and 0.7 nm (without additive, Figure 6a). This study indicates that polymers with different side chains show different sensitivities to the additive in photovoltaic performances. We are currently attempting to achieve optimal morphology and gain higher efficiency by varying the mixing solvents and/or processing additives.

CONCLUSION

Three conjugated copolymers bearing a common carbazole−thiophene−quinoxaline−thiophene polymer backbone but different side chains were designed and synthesized. The influence of the side chains on their photophysical, electrochemical, and photovoltaic properties was investigated. **EWC3**, bearing the most side chains, exhibited the best photovoltaic performance, and solar cells employing **EWC3**:[70]PCBM (1:3) as the photoactive layer showed the highest PCE of 3.7% and V_{oc} of 0.92 V. It was also noted that photovoltaic cells containing **EWC3**, with branched side chains on the carbazole units, gave much higher V_{oc} than devices containing **EWC1** with straight side chains on carbazole units. This study offered a useful and important guideline for designing 2,7-carbazole-based polymers for high performance PSCs.

EXPERIMENTAL SECTION

Characterization. ^{1}H NMR spectra were acquired from a Varian Inova 500 MHz NMR spectrometer. Tetramethylsilane was used as an internal reference with deuterated chloroform as solvent. TGA and DSC were performed on Perkin-Elmer TGA7 and Perkin-Elmer Pyris 1, respectively. Size exclusion chromatography (SEC) was performed on Waters Alliance GPCV2000 with a refractive index detector. Columns: Waters Styvagel HT GE × 1, Waters Styvagel HMW GE × 2. The eluent was 1,2,4-trichlorobenzene. The working temperature was 135 °C, and the resolution time was 2 h. The concentration of the samples was 0.5 mg mL^{-1}, which were filtered (filter: 0.45 μm) prior to the analysis. The molecular weights were calculated according to relative calibration with polystyrene standards. UV−vis absorption spectra were measured with a Perkin-Elmer Lambda 900 UV−vis−NIR absorption spectrometer. SWV measurements were carried out on a CH-Instruments 650A electrochemical workstation. A three-electrode setup was used with platinum wires, as both working electrode and counter electrode, and Ag/Ag$^+$ used as reference electrode calibrated with Fc/Fc$^+$. A 0.1 M solution of tetrabutylammonium hexafluorophosphate (Bu_4NPF_6) in anhydrous acetonitrile was used as supporting electrolyte. The polymers were deposited onto the working electrode from chloroform solution. In order to remove oxygen from the electrolyte, the system was bubbled with nitrogen prior to each experiment. The nitrogen inlet was then placed above the liquid surface and left there during the scans. HOMO and LUMO levels were estimated from peak potentials of the third scan.

Device Fabrication and Characterization. The structure of the solar cells was glass/ITO/PEDOT:PSS/active layer/LiF/Al. As a buffer layer, the conductive polymer, PEDOT:PSS (Baytron P VP Al 4083), was spin-coated onto ITO-coated glass substrates, followed by annealing at 120 °C for 10 min to remove water. The thickness of the PEDOT:PSS layer was about 45 nm, as determined by a Dektak 6 M surface profilometer. The active layer consisting of polymers and [70]PCBM was spin-coated from ODCB solution (or with DIO additive) onto the PEDOT:PSS layer. The spin-coating was done in a glovebox, and the material was directly transferred to a vapor deposition system mounted inside of the glovebox. LiF (0.6 nm) and Al (80 nm) were used as top electrodes and were deposited via a mask in vacuum onto the active layer. The accurate area of every device (4−6 mm^2), defined by the overlap of the ITO and metal electrode, was measured carefully by microscope image. EQEs were calculated from the photocurrents at short-circuit conditions. The currents were recorded by a Keithley 485 picoammeter under illumination of monochromatic light (MS257) through the ITO side of the devices. PCE was calculated from $J-V$ characteristics recorded by a Keithley 2400 source meter under illumination of an AM1.5G solar simulator with an intensity of 100 mW cm^{-2} (model SS-50A, Photo Emission Tech., Inc.). The light intensity was

determined by a standard silicon photodiode. Device characterization was conducted in ambient environment.

Synthesis of EWC1. In a 25 mL dry flask, monomer **1** (265 mg, 0.5 mmol), monomer **2** (431 mg, 0.5 mmol), Aliquat 336 (50 mg), tris(dibenzylideneacetone)dipalladium(0) ($Pd_2(dba)_3$) (5 mg), tri(*o*-tolyl)phosphine ($P(o\text{-}Tol)_3$) (10 mg), and K_3PO_4 (280 mg) were dissolved in a mixture of degassed toluene (8 mL) and deionized water (1 mL). The mixture was vigorously stirred at 100 °C for 4 h under nitrogen. The polymer was end-capped by adding 4,4,5,5-tetramethyl-2-phenyl-1,3,2-dioxaborolane (204 mg) and, after 2 h, bromobenzene (0.3 mL). The mixture was stirred for another 2 h, cooled down, and poured into acetone. The polymer was collected by filtration through 0.45 μm Teflon filter. It was then dissolved in ODCB (100 mL) and mixed with a solution of sodium diethyldithiocarbamate trihydrate (5 g) in deionized water (100 mL). The mixture was stirred at 80 °C overnight under nitrogen. The organic phase was separated and washed three times with water. Then it was poured into acetone (400 mL). The precipitate was collected and was Soxhlet-extracted in order with diethyl ether, dichloromethane, and then with chloroform. The chloroform solution was concentrated to a small volume, and the polymer was precipitated by pouring this solution into acetone. Finally, the polymer was collected by filtration using a 0.45 μm Teflon filter and dried under vacuum at 40 °C overnight (220 mg, 45%). ^{1}H NMR ($CDCl_3$, 500 MHz) δ: 8.17 (br, 2H), 7.93 (br, 2H), 7.61−7.43 (br, 14H), 6.99 (br, 2H), 4.33 (br, 2H), 3.86 (br, 4H), 1.92 (br, 4H), 1.31−1.14 (br, 32H), 0.83 (br, 9H).

Synthesis of EWC2. **EWC2** was prepared from monomer **3** (329 mg, 0.5 mmol) and monomer **4** (302 mg, 0.5 mmol) by following a similar procedure as described above for the synthesis of **EWC1**, but the reaction time was 2 h and the polymer was not washed by dichloromethane in Soxhlet extractor. The yield of **EWC2** was 170 mg (40%). ^{1}H NMR ($CDCl_3$, 500 MHz) δ: 8.18 (br, 2H), 7.86 (br, 4H), 7.61−7.44 (br, 16H), 4.69 (br, 1H), 2.43 (br, 4H), 2.04 (br, 4H), 1.29−1.13 (br, 20H), 0.76 (br, 6H).

Synthesis of EWC3. **EWC3** was prepared from monomer **3** (329 mg, 0.5 mmol) and monomer **2** (431 mg, 0.5 mmol) by using similar procedure as described above for synthesis of **EWC1**, but the reaction time was 24 h and the polymer was not washed by dichloromethane in Soxhlet extractor. The yield of **EWC3** was 402 mg (73%). ^{1}H NMR ($CDCl_3$, 500 MHz) δ: 8.19 (br, 2H), 8.08 (br, 2H), 7.89−7.32 (br, 14H), 6.97 (br, 2H), 4.67 (br, 1H), 3.87 (br, 4H), 2.39 (br, 4H), 2.03 (br, 8H), 1.29−1.15 (br, 40H), 0.85−0.78 (br, 12H).

AUTHOR INFORMATION

Corresponding Author

*E-mail: ergang@chalmers.se (E.W.); mats.andersson@chalmers.se (M.R.A.).

ACKNOWLEDGMENT

We thank the Swedish Energy Agency for financial support.

REFERENCES

(1) Coakley, K. M.; McGehee, M. D. *Chem. Mater.* **2004**, *16*, 4533.
(2) Gunes, S.; Neugebauer, H.; Sariciftci, N. S. *Chem. Rev.* **2007**, *107*, 1324.
(3) Hoppe, H.; Sariciftci, N. S. *J. Mater. Res.* **2004**, *19*, 1924.
(4) Cheng, Y. J.; Yang, S. H.; Hsu, C. S. *Chem. Rev.* **2009**, *109*, 5868.
(5) Yu, G.; Gao, J.; Hummelen, J. C.; Wudl, F.; Heeger, A. J. *Science* **1995**, *270*, 1789.
(6) Ma, W. L.; Yang, C. Y.; Gong, X.; Lee, K.; Heeger, A. J. *Adv. Funct. Mater.* **2005**, *15*, 1617.
(7) Li, G.; Shrotriya, V.; Huang, J. S.; Yao, Y.; Moriarty, T.; Emery, K.; Yang, Y. *Nature Mater.* **2005**, *4*, 864.
(8) Li, Y. F.; Zou, Y. P. *Adv. Mater.* **2008**, *20*, 2952.
(9) Chen, J. W.; Cao, Y. *Acc. Chem. Res.* **2009**, *42*, 1709.
(10) Park, S. H.; Roy, A.; Beaupre, S.; Cho, S.; Coates, N.; Moon, J. S.; Moses, D.; Leclerc, M.; Lee, K.; Heeger, A. J. *Nature Photonics* **2009**, *3*, 297.
(11) Chen, H. Y.; Hou, J. H.; Zhang, S. Q.; Liang, Y. Y.; Yang, G. W.; Yang, Y.; Yu, L. P.; Wu, Y.; Li, G. *Nature Photonics* **2009**, *3*, 649.
(12) Svensson, M.; Zhang, F. L.; Veenstra, S. C.; Verhees, W. J. H.; Hummelen, J. C.; Kroon, J. M.; Inganäs, O.; Andersson, M. R. *Adv. Mater.* **2003**, *15*, 988.
(13) Wang, E. G.; Wang, L.; Lan, L. F.; Luo, C.; Zhuang, W. L.; Peng, J. B.; Cao, Y. *Appl. Phys. Lett.* **2008**, *92*, 033307.
(14) Zhang, F. L.; Mammo, W.; Andersson, L. M.; Admassie, S.; Andersson, M. R.; Inganäs, O. *Adv. Mater.* **2006**, *18*, 2169.
(15) Blouin, N.; Michaud, A.; Leclerc, M. *Adv. Mater.* **2007**, *19*, 2295.
(16) Chu, T. Y.; Alem, S.; Verly, P. G.; Wakim, S.; Lu, J. P.; Tao, Y.; Beaupre, S.; Leclerc, M.; Belanger, F.; Desilets, D.; Rodman, S.; Waller, D.; Gaudiana, R. *Appl. Phys. Lett.* **2009**, *95*, 063304.
(17) Gadisa, A.; Mammo, W.; Andersson, L. M.; Admassie, S.; Zhang, F.; Andersson, M. R.; Inganäs, O. *Adv. Funct. Mater.* **2007**, *17*, 3836.
(18) Lindgren, L. J.; Zhang, F. L.; Andersson, M.; Barrau, S.; Hellstrom, S.; Mammo, W.; Perzon, E.; Inganäs, O.; Andersson, M. R. *Chem. Mater.* **2009**, *21*, 3491.
(19) Wang, E. G.; Hou, L. T.; Wang, Z. Q.; Hellström, S.; Zhang, F. L.; Inganäs, O.; Andersson, M. R. *Adv. Mater.* **2010**, *22*, 5240.
(20) Zhou, E.; Cong, J. Z.; Tajima, K.; Hashimoto, K. *Chem. Mater.* **2010**, *22*, 4890.
(21) Wang, E. G.; Wang, M.; Wang, L.; Duan, C. H.; Zhang, J.; Cai, W. Z.; He, C.; Wu, H. B.; Cao, Y. *Macromolecules* **2009**, *42*, 4410.
(22) Zoombelt, A. P.; Leenen, M. A. M.; Fonrodona, M.; Nicolas, Y.; Wienk, M. M.; Janssen, R. A. J. *Polymer* **2009**, *50*, 4564.
(23) Piliego, C.; Holcombe, T. W.; Douglas, J. D.; Woo, C. H.; Beaujuge, P. M.; Fréchet, J. M. J. *J. Am. Chem. Soc.* **2010**, *132*, 7595.
(24) Thompson, B. C.; Kim, B. J.; Kavulak, D. F.; Sivula, K.; Mauldin, C.; Fréchet, J. M. J. *Macromolecules* **2007**, *40*, 7425.
(25) Liang, Y. Y.; Feng, D. Q.; Wu, Y.; Tsai, S. T.; Li, G.; Ray, C.; Yu, L. P. *J. Am. Chem. Soc.* **2009**, *131*, 7792.
(26) Szarko, J. M.; Guo, J.; Liang, Y.; Lee, B.; Rolczynski, B. S.; Strzalka, J.; Xu, T.; Loser, S.; Marks, T. J.; Yu, L.; Chen, L. X. *Adv. Mater.* **2010**, *22*, 5468.
(27) Yang, L.; Zhou, H.; You, W. *J. Phys. Chem. C* **2010**, *114*, 16793.
(28) Biniek, L.; Fall, S.; Chochos, C. L.; Anokhin, D. V.; Ivanov, D. A.; Leclerc, N.; Lévêque, P.;; Heiser, T. *Macromolecules* **2010**, *43*, 9779.
(29) Zotti, G.; Schiavon, G.; Zecchin, S.; Morin, J.-F.; Leclerc, M. *Macromolecules* **2002**, *35*, 2122.
(30) Bijleveld, J. C.; Zoombelt, A. P.; Mathijssen, S. G. J.; Wienk, M. M.; Turbiez, M.; de Leeuw, D. M.; Janssen, R. A. J. *J. Am. Chem. Soc.* **2009**, *131*, 16616.
(31) Zhu, Z.; Waller, D.; Gaudiana, R.; Morana, M.; Mühlbacher, D.; Scharber, M.; Brabec, C. *Macromolecules* **2007**, *40*, 1981.
(32) Wang, E. G.; Hou, L. T.; Wang, Z. Q.; Hellstrom, S.; Mammo, W.; Zhang, F. L.; Inganäs, O.; Andersson, M. R. *Org. Lett.* **2010**, *12*, 4470.
(33) Scharber, M. C.; Wuhlbacher, D.; Koppe, M.; Denk, P.; Waldauf, C.; Heeger, A. J.; Brabec, C. J. *Adv. Mater.* **2006**, *18*, 789.
(34) Hellström, S.; Zhang, F. L.; Inganäs, O.; Andersson, M. R. *Dalton Trans.* **2009**, 10032.
(35) Mammo, W.; Admassie, S.; Gadisa, A.; Zhang, F. L.; Inganäs, O.; Andersson, M. R. *Sol. Energy Mater. Sol. Cells* **2007**, *91*, 1010.
(36) Pavlishchuk, V. V.; Addison, A. W. *Inorg. Chim. Acta* **2000**, *298*, 97.
(37) Bard, A. J.; Faulkner, L. R. *Electrochemical Methods: Fundamentals and Applications*, 2nd ed.; Wiley: New York, 2001.

(38) Wienk, M. M.; Kroon, J. M.; Verhees, W. J. H.; Knol, J.; Hummelen, J. C.; van Hal, P. A.; Janssen, R. A. J. *Angew. Chem., Int. Ed.* **2003**, *42*, 3371.
(39) Blouin, N.; Leclerc, M. *Acc. Chem. Res.* **2008**, *41*, 1110.
(40) Qin, R. P.; Li, W. W.; Li, C. H.; Du, C.; Veit, C.; Schleiermacher, H. F.; Andersson, M.; Bo, Z. S.; Liu, Z. P.; Inganäs, O.; Wuerfel, U.; Zhang, F. L. *J. Am. Chem. Soc.* **2009**, *131*, 14612.
(41) Liang, Y. Y.; Xu, Z.; Xia, J. B.; Tsai, S. T.; Wu, Y.; Li, G.; Ray, C.; Yu, L. P. *Adv. Mater.* **2010**, *22*, E135.
(42) Hoppe, H.; Sariciftci, N. S. *J. Mater. Chem.* **2006**, *16*, 45.
(43) Lee, J. K.; Ma, W. L.; Brabec, C. J.; Yuen, J.; Moon, J. S.; Kim, J. Y.; Lee, K.; Bazan, G. C.; Heeger, A. J. *J. Am. Chem. Soc.* **2008**, *130*, 3619.
(44) Peet, J.; Kim, J. Y.; Coates, N. E.; Ma, W. L.; Moses, D.; Heeger, A. J.; Bazan, G. C. *Nature Mater.* **2007**, *6*, 497.
(45) Clarke, T. M.; Durrant, J. R. *Chem. Rev.* **2010**, *110*, 6736.